**Advances in Concrete Construction**, *Vol. 11, No. 6 (2021) 469-479*
DOI: https://doi.org/10.12989/acc.2021.11.6.469


# Effect of plastic rotation on the concrete contribution to shear strength of RC beams

Cem Aydemir*[1], Müberra Eser Aydemir[1a] and Güray Arslan[2b]

*[1]Department of Civil Engineering, İstanbul Aydın University, İstanbul, Turkey*
*[2]Department of Civil Engineering, Yıldız Technical University, İstanbul, Turkey*

(*Received September 18, 2020, Revised April 21, 2021, Accepted April 28, 2021*)

**Abstract.** This paper provides an analytical model to predict the concrete contribution to shear strength of reinforced concrete (RC) beams that fail in flexure. In the RC members subjected to cyclic loading, the stiffness and hysteretic energy dissipation decreases with diagonal web cracking in the plastic hinge region. The proposed method takes into account plastic rotation in the plastic hinge region by means of critical shear crack theory. To verify the concrete contribution to shear strength predicted by the proposed method, six normal- and high-strength RC beams having various shear span-to-effective depth ratios are tested under cyclic loading. The predictions by the proposed equation and various researchers' equations are compared to the test results. It is found that the proposed method is in good agreement with the test results.

**Keywords:** degradation in the shear strength; seismic performance; RC beams; concrete contribution; high-strength concrete; plastic hinge rotation

## 1. Introduction

The degradation in the shear strength of reinforced concrete (RC) members has been the subject of many controversies and debates for the past four decades. Bousias *et al*. (1995) and Acun and Sucuoglu (2012) stated that RC members are unable to maintain their properties under cyclic loading in comparison with monotonic loading and cyclic loading causes larger inelastic deformation demands and damage accumulation. The shear strength degradation of RC members under cyclic lateral loading occurs faster than the flexural strength degradation (Biskinis *et al*. 2004 and Keskin 2017). Hence, the reduction in the shear capacity due to cyclic loading should be taken into account while designing RC structures or assessing the existing RC members. Park *et al*. (2012) also indicated that previous models are based on experimental data and field observations of earthquake damaged buildings since the shear strength degradation is a complex phenomenon.

Shear strength degradation occurs in RC beams that exhibit flexural yielding during cyclic loading (Aydemir and Eser Aydemir 2020). Several models have been developed to represent the degradation of RC members with increasing deformations (Ascheim and Moehle 1992, Priestly *et al*. 1994, Pérez and Pantazopoulou 1998, Kowalsky and Priestley 2000, Elwood and Moehle 2005), longitudinal strain (Muttoni and Fernández 2008), depth of the compression zone (Olalusi 2019, Campione *et al*. 2014). Moehle *et al*. (2001) and Sezen and Moehle (2004) proposed that the shear strength of RC columns is related to the displacement ductility demand. The reduction of shear strength with cyclic rotations is considered to affect both the contribution of transverse reinforcement, based on 45 degree truss model, and the contribution of concrete, which are multiplied by the same coefficient. Aschheim and Moehle (1992), Priestly *et al*. (1994), and Pérez and Pantazopoulou (1998) proposed a degradation coefficient for the contribution of concrete, which is determined by the displacement ductility. Lee and Watanabe (2003) predicted the shear degradation of RC beams after flexural yielding by using a compatibility-aided truss model. Based on the experimental results, Elwood and Moehle (2005) developed a drift capacity model for the displacement-based design and assessment of existing structures. Arslan (2005) proposed a model for degradation coefficient by considering that the contribution of concrete to shear strength is zero, and the shear strength is provided by merely transverse reinforcement at collapse. Kowalsky and Priestley (2000) proposed a revised version of UCSD (University of California, San Diego) shear model, where the reduction in the concrete contribution to the shear strength depends on the column aspect ratio, longitudinal steel ratio and displacement ductility. De Domenico and Ricciardi G. (2020) proposed a model is based on the concept of cracked membrane element combined with the variable strut inclination method of the Eurocode 2. Advanced, structural-mechanics-based shear models like the modified compression field theory (Vecchio and Collins 1986, Vecchio *et al*. 2008, Sezen 2008) or the axial-shear-flexure interaction approach (Mostafaei *et al*. 2009) have proven to be rather accurate, but these approaches involve

*Corresponding author, Associate Professor
E-mail: cemaydemir@aydin.edu.tr
[a]Professor
E-mail: muberraaydemir@aydin.edu.tr
[b]Professor
E-mail: aguray@yildiz.edu.tr


http://www.techno-press.org/?journal=acc&subpage=7
ISSN: 2287-5301 (Print), 2287-531X (Online)

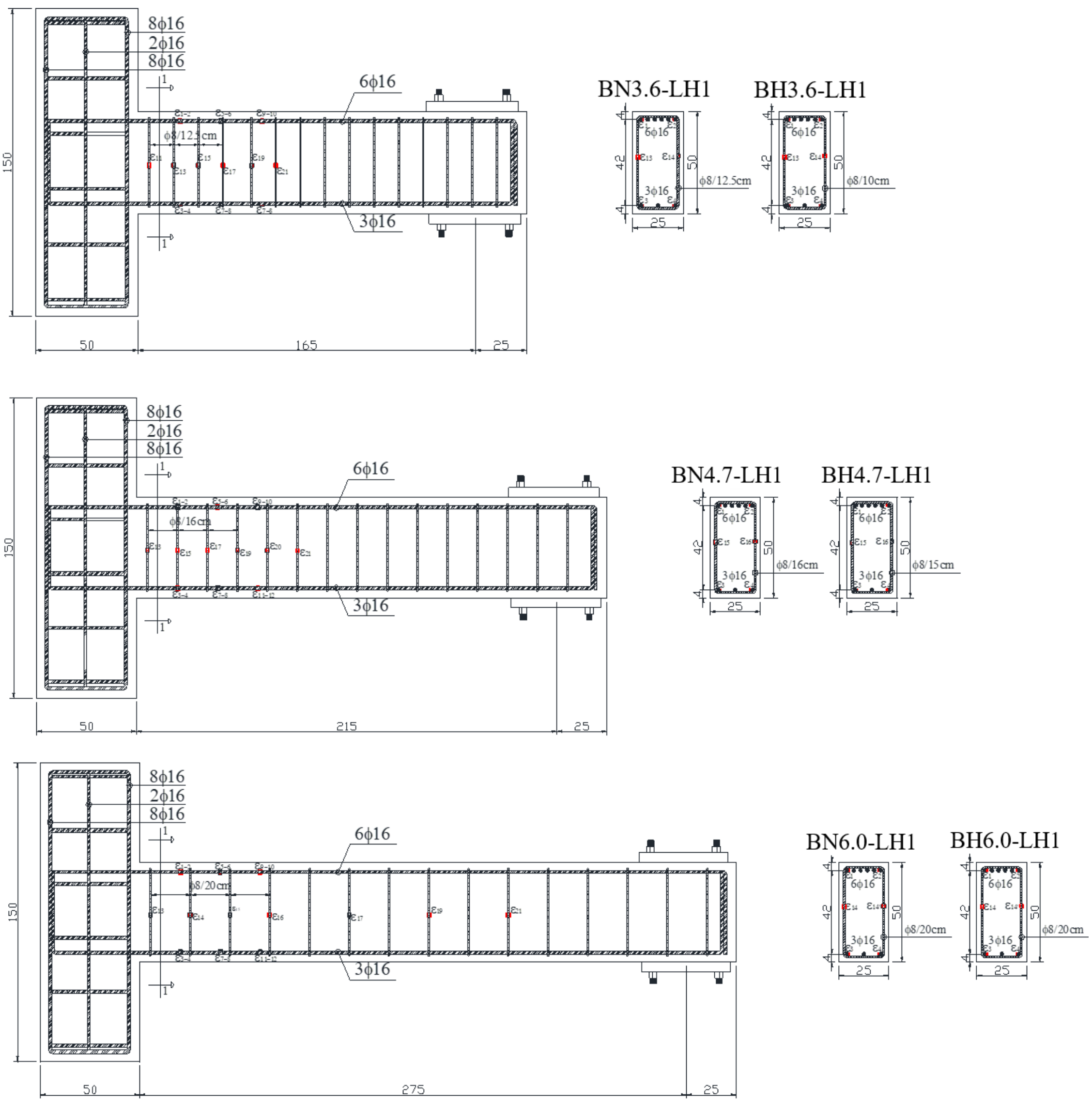


Fig. 1 Geometry, detailing and instrumentation of the specimens

high computational demand (Zimos *et al*. 2018).

Most of the previous studies were mainly focused on the behaviour of RC members subjected to a shear-dominant seismic loading condition. This paper considers the test results of RC beams under a flexural-dominant loading condition. Such a loading condition is common for beams in multistory frame structures subjected to lateral loading. Common practices using a ductile design approach based on the strong column-weak beam mechanism require proper designs of columns against any shear failure. Moreover, a beam mechanism in which yielding takes place at the beam ends is realistic for multistory frame structures under cyclic loading. The shear strength of RC members is decreased by diagonal cracking under cyclic loading as the plastic rotation increases. In the present study, a new approach is developed based on the influence of plastic rotation on the concrete contribution to shear strength using critical shear crack theory. For verification, the predictions by the proposed model and various researchers' models are compared with the test results of this study.

## 2. Experimental program

### 2.1 Specimens

Six cantilever RC beams were tested under cyclic loading. For the cantilever specimens, loading point represents the zero moment point whereas the support of cantilever beam corresponds to a rigid column in an actual structure. The geometry and details of specimens are illustrated in Fig. 1, whereas significant section properties are presented in Table 1. All beams are 250 mm wide (b), and 500 mm high (h), with an effective depth (d) of 460 mm and shear span-to-effective depth ratios (*a/d*) ranging from 3.6 to 6.0. The shear reinforcement was calculated as (diameter/spacing) $\phi$8/12.5, $\phi$8/16 and $\phi$8/20 for shear span-to-effective depth ratios 3.6, 4.7 and 6.0, respectively, to ensure flexural rather than shear failure. The top and bottom flexural reinforcement were used as 6$\phi$16 and 3$\phi$16, respectively. The cross-sectional dimensions and reinforcement layouts of beams are shown in Fig. 1.

Table 1 Specimen properties

| | Parameter | Specimens | | | | | |
|---|---|---|---|---|---|---|---|
| | | BN3.6-LH1 | BN4.7-LH1 | BN6.0-LH1 | BH3.6-LH1 | BH4.7-LH1 | BH6.0-LH1 |
| *Geometric* | *b/h/d* (cm/cm/cm) | 25/50/46 | 25/50/46 | 25/50/46 | 25/50/46 | 25/50/46 | 25/50/46 |
| | (*a/d*) (cm/cm) | 165/46=3.6 | 215/46=4.7 | 275/46=6.0 | 165/46=3.6 | 215/46=4.7 | 275/46=6.0 |
| *Material* | $f'_c$ (MPa) | 45.6 | 46.9 | 48.6 | 64.4 | 68.4 | 65.4 |
| | $f_y/f_{su}/f_{yw}$ (MPa) | 498/602/597 | 498/602/597 | 498/602/597 | 498/602/597 | 498/602/597 | 498/602/597 |
| | $\varepsilon_{sh}/\varepsilon_{su}$ | 0.009/0.14 | 0.009/0.14 | 0.009/0.14 | 0.009/0.14 | 0.009/0.14 | 0.009/0.14 |
| *Reinforcement* | Top flexural reinforcement (ratio) | 6$\phi$16 (0.0105) | 6$\phi$16 (0.0105) | 6$\phi$16 (0.0105) | 6$\phi$16 (0.0105) | 6$\phi$16 (0.0105) | 6$\phi$16 (0.0105) |
| | Bottom flexural reinforcement (ratio) | 3$\phi$16 (0.0052) | 3$\phi$16 (0.0052) | 3$\phi$16 (0.0052) | 3$\phi$16 (0.0052) | 3$\phi$16 (0.0052) | 3$\phi$16 (0.0052) |
| | Shear reinforcement (ratio) | $\phi$8/12.5 (0.0032) | $\phi$8/16 (0.0025) | $\phi$8/20 (0.002) | $\phi$8/12.5 (0.0032) | $\phi$8/16 (0.0025) | $\phi$8/20 (0.002) |

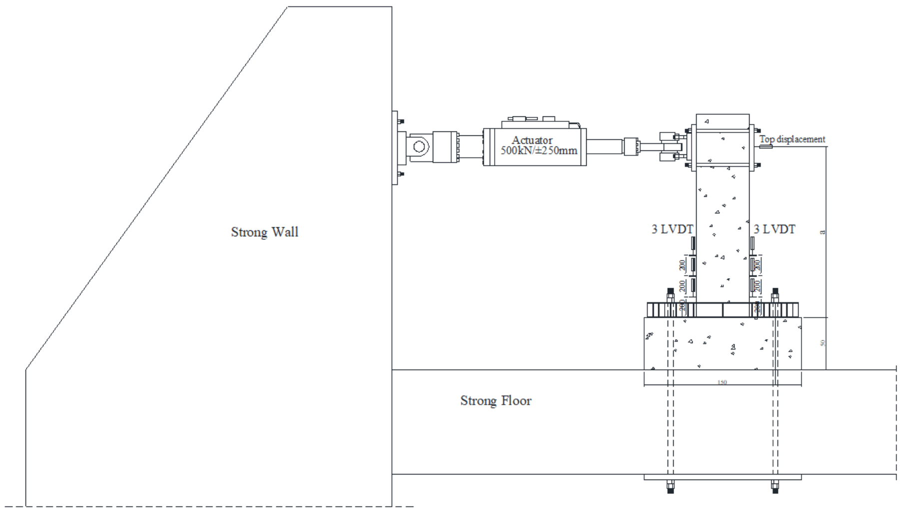


Fig. 2 Test configuration

Transverse reinforcement design of test specimens is completed based on the capacity design approach. The ratio of maximum shear force to lateral reinforcement shear strength ($V_{\max}/V_s$) for test specimens are designed approximately to be equal (See Table 2). Besides, it is worth to note that, for specimens with *a/d* ratio of 3.6, spacing of lateral reinforcement sustains Turkish Seismic Design Code (TSDC-2007) requirements ($s \leq h/4$, $s \leq 8\phi_l$, $s \leq 15$ cm) whereas for specimens with *a/d* ratio of 6.0 this statement is not valid. The beams were designated regarding to compressive strength of concrete ($f'_c$), shear span-to-effective depth ratio and load history. The beam designation includes a combination of letters and numbers: BN or BH to indicate the compressive strength of concrete; 3.6, 4.7 or 6.0 to indicate the shear span-to-effective depth ratio; and LH1 to designate the 1$^{st}$ load history. For example, a beam made of high strength concrete having a shear span-to-effective depth ratio of 3.6 and LH1 is labelled as BH3.6-LH1. All longitudinal bars have an average yield strength ($f_y$) of 480 MPa, and an average tensile strength ($f_{su}$) of 725 MPa. Shear reinforcement bars have an average yield strength ($f_{yw}$) of 597 MPa. All bars have a yield strain in the beginning of strain hardening ($\varepsilon_{sh}$) and a rupture strain ($\varepsilon_{su}$) of 0.009 and 0.14, respectively.

### *2.2 Test setup*

The test specimens were tested at the Structural Testing Laboratory of Istanbul Aydin University. A sample cantilever specimen in the test configuration is shown schematically in Fig. 2. Prior to testing, the specimen was supported to the laboratory strong floor by anchor blocks to prevent sliding and overturning and a double-acting pseudo-controlled 500 kN (±250 mm) capacity actuator was connected to the load arm. 30-channel Data loggers were used for data acquisition.

Six linear variable displacement transducers (LVDTs) were attached on the side surfaces of each beam to measure the plastic rotation (see Fig. 2). In order to monitor the development of strain in the longitudinal reinforcement and shear reinforcement with progressive loading, electrical strain gauges were installed. A computer aided data acquisition system automatically monitored load, displacements and strains at pre-selected time intervals. The

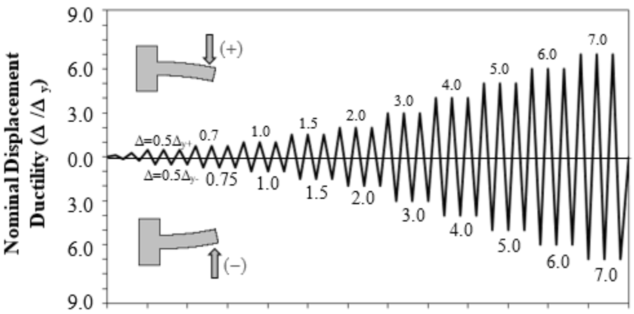


Fig. 3 Target nominal displacement ductility history ($+\Delta_y \neq -\Delta_y$)

tests also provided information on the behavior of beams including development of cracks, crack patterns, and failure modes.

### 2.3 Loading procedure

The loading history, LH1 contains standard cyclic loading procedure with an increasing displacement amplitude. All specimens were subjected to similar loading procedures. The target lateral displacement history was based on nominal displacement ductility ($\Delta/\Delta_{y,\ analytical}$) as presented in Fig. 3. Three cycles were run for each nominal displacement ductility amplitude, followed by a single cycle for post-yield cycles.

## 3. Test results and discussion

### 3.1 Failure modes

The maximum shear demand, the shear force corresponding to the development of the flexural strength of beam, the shear strength calculated according to ACI-318 (2014) and the failure mode for each beam are listed in Table 2. Experimental material strengths are used for moment and shear force capacities, whereas concrete

Table 2 Comparison of flexural and shear capacities

| Specimens/ Direction | | $V_{max}$(1) | $V_f$(2) | $V_w$(3) | $V_{max}/V_f$ | $V_{max}/V_w$ | Failure Mode(4) |
|---|---|---|---|---|---|---|---|
| BN3.6-LH1 | + | 159 | 155.9 | 220.8 | 1.02 | 0.72 | F/T |
| | - | 84.5 | 80.5 | 220.8 | 1.05 | 0.38 | F/T |
| BN4.7-LH1 | + | 119.5 | 119.4 | 184.0 | 1.00 | 0.65 | F/T |
| | - | 65.2 | 61.9 | 184.0 | 1.05 | 0.35 | F/T |
| BN6.0-LH1 | + | 95.2 | 94.3 | 138.0 | 1.01 | 0.69 | F/T |
| | - | 50.4 | 48.5 | 138.0 | 1.04 | 0.37 | F/T |
| BH3.6-LH1 | + | 164.6 | 159.8 | 220.8 | 1.03 | 0.75 | F/T |
| | - | 84.8 | 81.5 | 220.8 | 1.04 | 0.38 | F/T |
| BH4.7-LH1 | + | 117.3 | 121.9 | 184.0 | 0.96 | 0.64 | F/T |
| | - | 66.5 | 64.5 | 184.0 | 1.03 | 0.36 | F/T |
| BH6.0-LH1 | + | 96.3 | 95.3 | 138.0 | 1.01 | 0.70 | F/T |
| | - | 50.4 | 48.9 | 138.0 | 1.03 | 0.37 | F/T |

(1): Maximum shear demand
(2): Shear force corresponding to the development of the flexural strength of beam calculated with experimental materials strength
(3): Transverse reinforcement shear strength calculated with experimental yield strength ($V_w=A_{sw}f_{yw}d/s$)
(4): F/T is Tension-controlled flexural failure

contribution is neglected (ACI 318-14) for shear capacities of test samples. The shear force corresponding to the development of the flexural strength of beam ($V_f$) were determined by Eq. (1).

$$V_f = \frac{M_f}{a} \tag{1}$$

where $M_f$ is the flexural strength assuming a strength reduction factor $\phi$ of 1.0 and a is the clear span length of the cantilever beam. The shear force corresponding to the development of the shear strength of beam ($V_w$) were determined by following Eq. (2), assuming the concrete contribution to shear strength ($V_c$) was ignored (ACI 318 2014, and TSDC (2007).

$$V_w = \frac{A_v f_{yw} d}{s} \tag{2}$$

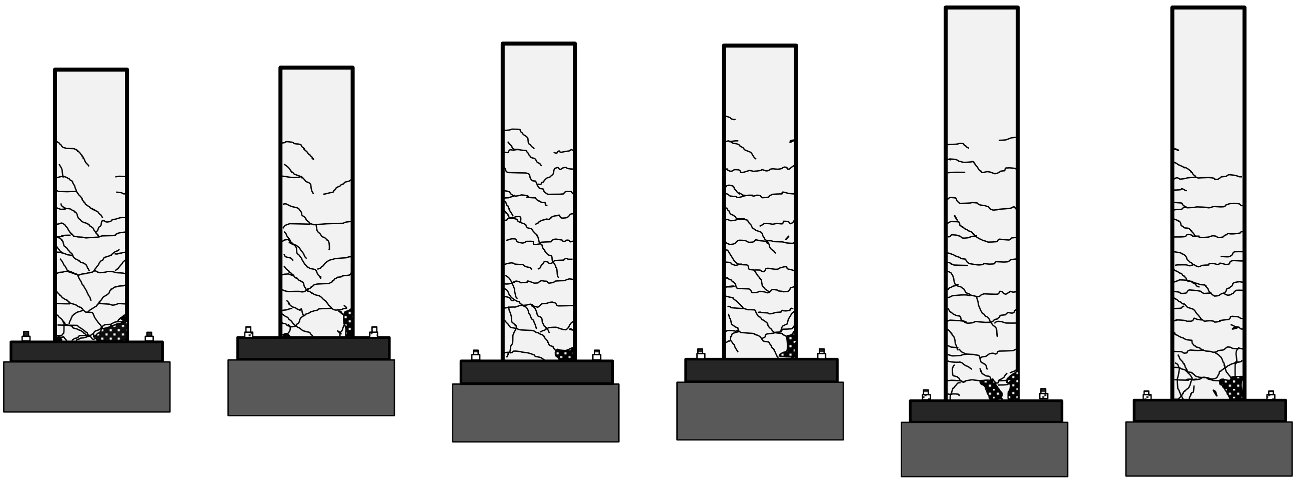

(a) BN3.6-LH1 (b) BH3.6-LH1 (c) BN4.7-LH1 (d) BH4.7-LH1 (e) BN6.0-LH1 (f) BH6.0-LH1

Fig. 4 Crack patterns of all test beams at failure

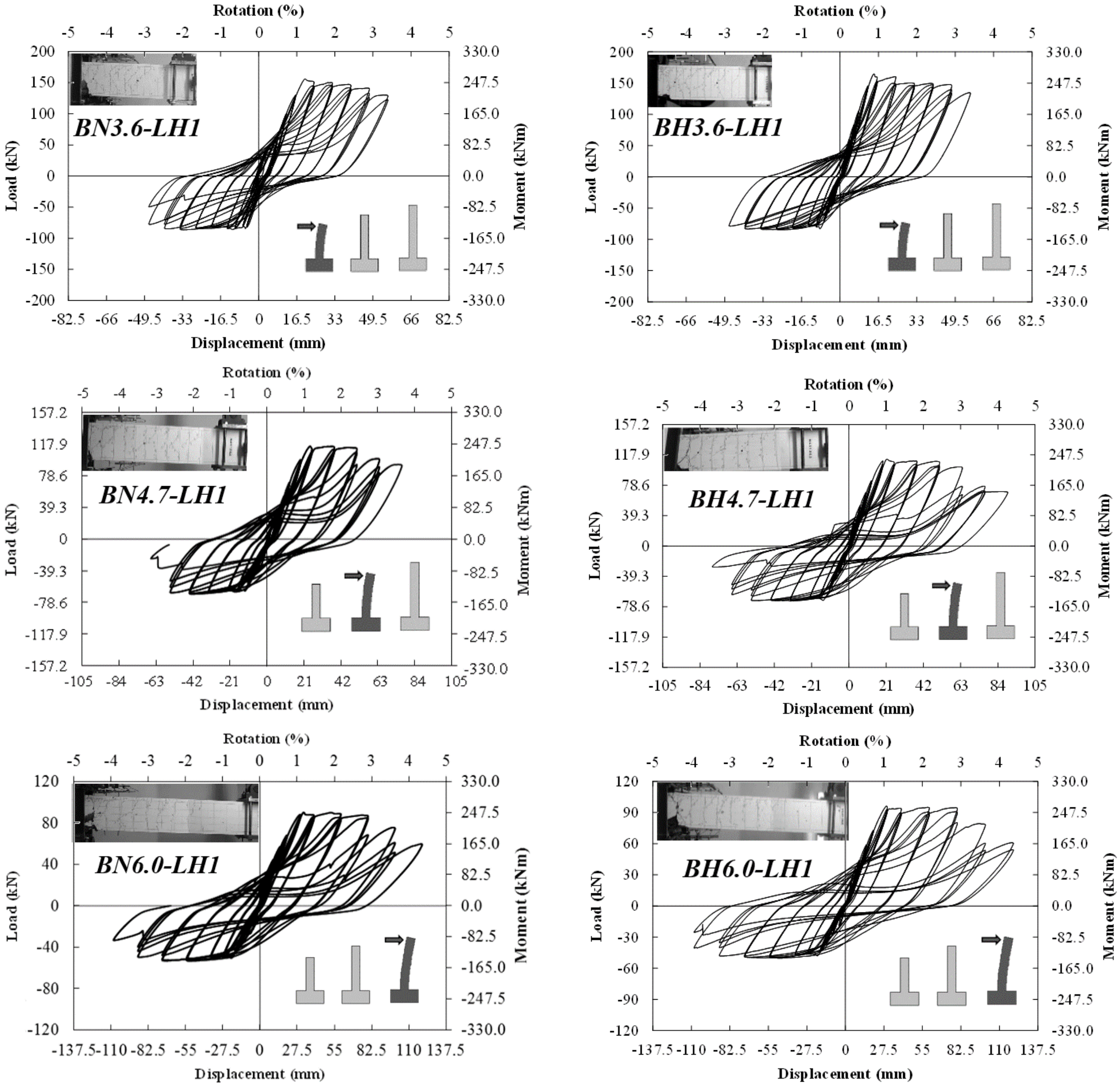


Fig. 5 Force-displacement response of test specimens

where $A_v$ is the $s$ the area of shear reinforcement, $f_{yw}$ is the experimental yield strength of shear reinforcement, $d$ is the effective depth of the beam section and $s$ is spacing of shear reinforcement.

Fig. 4 presents schematic diagrams and crack patterns of all test beams at failure. As expected, during the early stages of loading, fine vertical flexural cracks appeared around the fixed end of all of the beams. With increase in load, new flexural cracks formed extending from the fixed end through the free end. With a further increase, some of the flexural cracks started to propagate diagonally, and other new flexural cracks began to form separately farther away from the fixed end of the beam. In all beams, flexural failure occurred after a diagonal shear crack extended to the top fibre, as indicated in Fig. 4.

### 3.2 Force-displacement response

Load-displacement and moment-rotation relations for all beams are presented in Fig. 5. As shown in Fig. 5 and Table 2, an increase in the *a/d* leads to increase in displacement

Table 3 Shear strength and displacement ductility at diagonal cracking for test specimens

| Specimens/Direction | | *a/d* | $\rho^{(1)}$ | $\rho'^{(2)}/\rho$ | $V_{cr}^{(3)}$ (kN) | $\mu_{Vcr}^{(4)}$ |
|---|---|---|---|---|---|---|
| BN3.6-LH1 | + | 3.6 | 0.0105 | 0.5 | 155.8 | 1.26 |
| | - | 3.6 | 0.0052 | 2.0 | -82.0 | 3.40 |
| BN4.7-LH1 | + | 4.7 | 0.0105 | 0.5 | 112.6 | 1.33 |
| | - | 4.7 | 0.0052 | 2.0 | -63.8 | 3.82 |
| BN6.0-LH1 | + | 6.0 | 0.0105 | 0.5 | 87.0 | 1.67 |
| | - | 6.0 | 0.0052 | 2.0 | N/O | N/O |
| BH3.6-LH1 | + | 3.6 | 0.0105 | 0.5 | 159.4 | 1.61 |
| | - | 3.6 | 0.0052 | 2.0 | -78.5 | 4.01 |
| BH4.7-LH1 | + | 4.7 | 0.0105 | 0.5 | 109.9 | 1.35 |
| | - | 4.7 | 0.0052 | 2.0 | -70.4 | 3.14 |
| BH6.0-LH1 | + | 6.0 | 0.0105 | 0.5 | 94.9 | 1.78 |
| | - | 6.0 | 0.0052 | 2.0 | -50.0 | 4.44 |

Note: N/O is the abbreviation for "Not Observed"
(1): Tension reinforcement ratio, $A_s/(b_w \times d)$.
(2): Compression reinforcement ratio, $A_{s'}/(b_w \times d)$.
(3): $V_{cr}$ is shear force at diagonal crack was observed.
(4): $\mu_{Vcr}$ is displacement ductility factor at diagonal crack was observed.

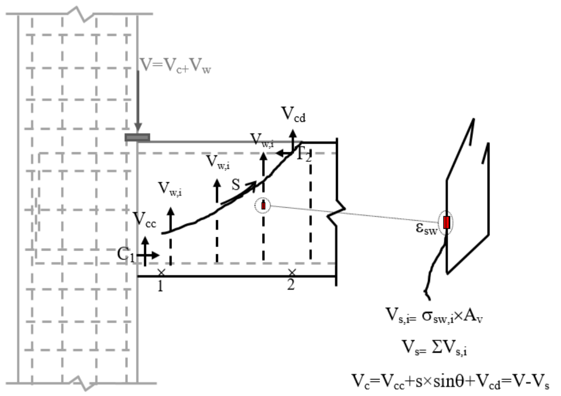


Fig. 6 Components of shear resistance and determination of $V_s$ and $V_c$ at critical diagonal crack of beam

and rotation and decrease in load and moment capacity.

### *3.3 Variation in $V_s$ and $V_c$ at observed damage states*

Diagonal crack strength of test samples ($V_{cr}$) and displacement ductility ratios for diagonal crack formation ($\mu_{Vcr}$) are summarized in Table 3. Diagonal crack formation of each test sample is obtained by visual investigation in each step of target maximum value of displacement history. As it can be seen from diagonal crack strength and displacement ductility ratio relationships given in Fig. 3, increase in *a/d* ratio of beam samples leads to not only decrease in diagonal cracking strength but also increase in ductility ratio.

For a reinforced concrete beam under cyclic moment and shear force, both reversing flexural and shear damages would occur due to displacement demand. A schematical view of only one direction diagonal shear crack is presented in Fig. 6 to represent shear force components of a reinforced concrete beam section briefly. As the vertical force equilibrium is considered, shear resistance of the section can be defined as the sum of concrete contribution and lateral reinforcement contribution. Lateral reinforcement contribution is equal to total of shear forces at lateral reinforcements that cross the diagonal shear cracks. Thus, concrete contribution is the sum of shear strength component from the concrete in the uncracked

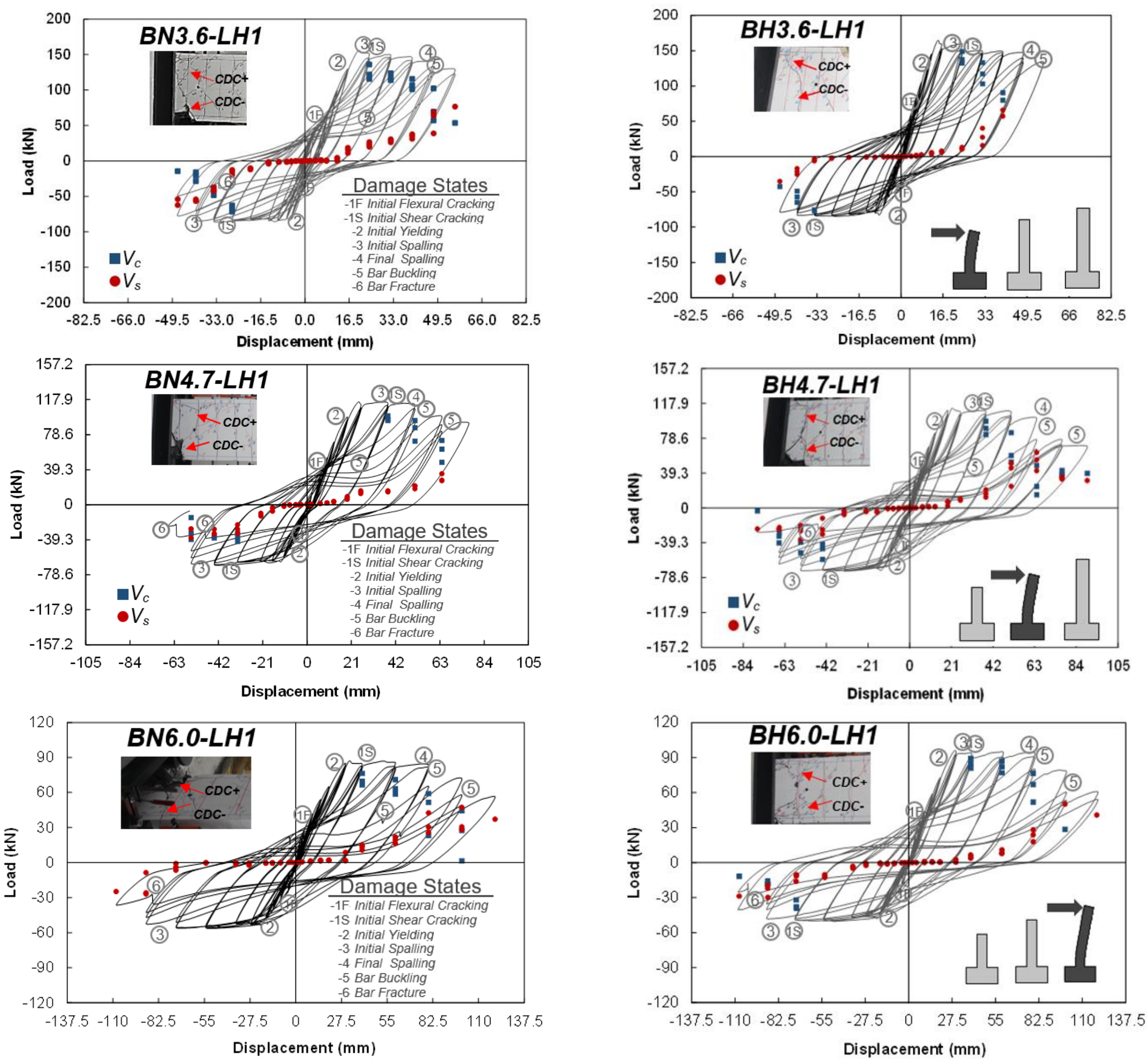


Fig. 7 Variation in $V_c$ and $V_s$ at critical diagonal crack (CDC) of test specimens

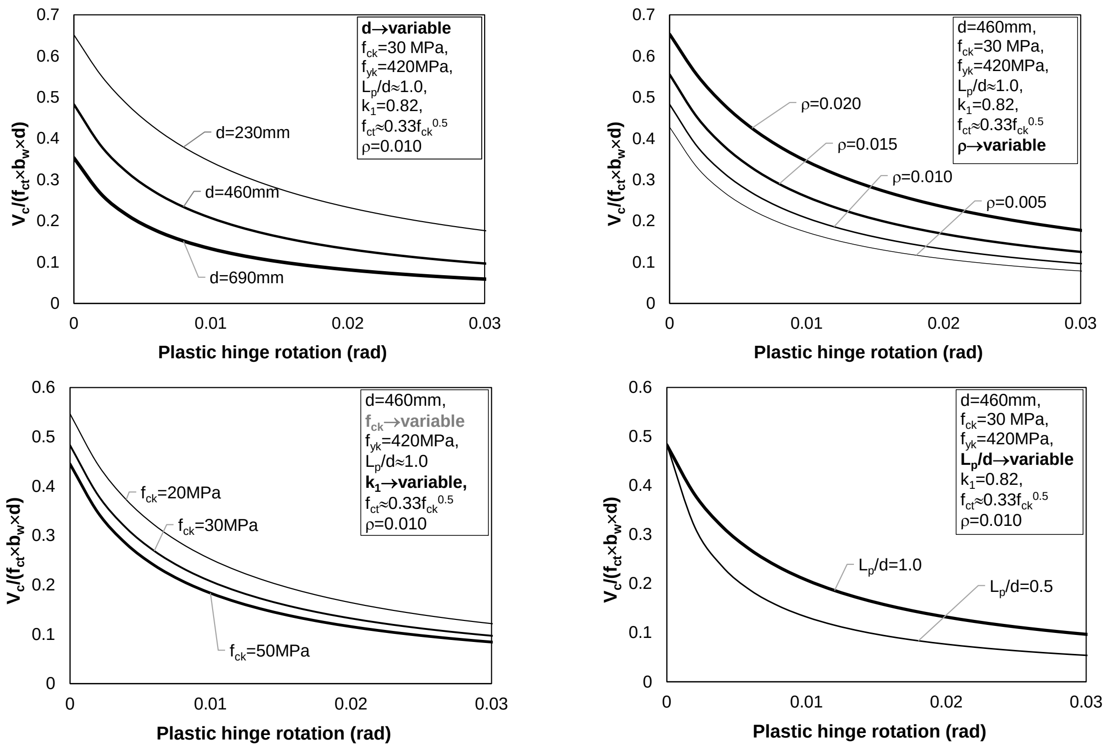


Fig. 8 Variation of concrete contribution of shear strength with different parameters

compression zone, the aggregate interlock and dowel action, respectively.

Shear forces of lateral reinforcement in test samples are obtained with the aid of experimental strains. Shear contribution of lateral reinforcements at a critical crack observed on a beam specimen under cyclic loading is defined as the sum of shear forces at lateral reinforcements that cross the diagonal shear crack. For the observed diagonal crack, concrete contribution to shear strength is obtained as the difference between the experimental shear force and lateral reinforcement shear contribution. Variation of concrete contribution and lateral reinforcement contribution to shear resistance with displacement demand for the observed critical shear crack is presented in Fig. 7. In addition, various damage states observed during the experiments are also illustrated in the figures to gain a better understanding for the damage state of beam support. The most notable observations, in sequence of first occurrence, are concrete flexural cracking, longitudinal reinforcement yielding, and initial spalling of the concrete cover, initial diagonal cracking, complete spalling of the concrete cover, longitudinal reinforcement buckling, and longitudinal reinforcement fracture.

## 4. Influence of plastic rotation on the concrete contribution to shear strength

Variation of concrete contribution to shear strength with displacement demand for sample beams has been investigated in Sec. 3.3. Critical shear crack theory will be used to investigate the relation between the mentioned variation and plastic hinge rotation of RC beams. Concrete contribution to shear strength according to critical shear crack theory (Muttoni 2008) can be expressed as

$$\frac{V_c}{b_w d\sqrt{f_c'}} = \frac{1}{6}\frac{2}{1+\dfrac{120\varepsilon_{0.6d}\,d}{16+d_g}} \quad (mm, MPa) \tag{3}$$

where $f_c$ is concrete compressive strength, $\varepsilon_{0.6d}$ is longitudinal strain at the fiber from $0.6d$ to exterior compression side at shear critical section, d is effective depth and dg is maximum size of aggregate. $\varepsilon_{0.6d}$ value corresponding to longitudinal strain at control depth can be defined as

$$\varepsilon_{0.6d}\,d = \phi d^2\left(0.6-\frac{x}{d}\right) \tag{4}$$

where $x$ is neutral axis depth, $\phi$ is total curvature at critical section. As the right side of Eq. (4) is multiplied by $L_p/L_p$ and rewriting the ($\phi=\phi_y+\phi_p$), ($\theta_p=\phi_p L_p$), ($\phi_y=c\varepsilon_y/h$) (Priestley 2000) equalities for elastic beyond shear critical section, shear resistance of concrete is defined with Eq. (5).

$$V_c = \frac{0.33\sqrt{f_c'}\,b_w\,d}{1+\dfrac{1.5\left(\theta_p+1.85\varepsilon_{sy}\dfrac{L_p}{d}\right)d^2\left(0.6-\dfrac{x}{d}\right)}{L_p}} \quad (mm, MPa) \tag{5}$$

Using the equality of compressive and tensile forces of singly reinforced rectangular beams, neutral axis depth can be defined based on mechanical reinforcement ratio ($\omega=\rho f_y/f_c$) and equivalent stress block parameter for concrete ($k_1$) as given below

$$\frac{x}{d} \approx \frac{\omega}{0.85k_1} \quad (6)$$

As Eq. (6) is rewritten in Eq. (5), concrete contribution of shear force is defined based on plastic rotation capacity

$$V_c = \frac{0.33\sqrt{f_c'}\,b_w\,d}{1+\dfrac{1.5\left(\theta_p + 1.85\varepsilon_{sy}\dfrac{L_p}{d}\right)d^2\left(0.6-\dfrac{\omega}{0.85k_1}\right)}{L_p}} \;(mm, MPa) \quad (7)$$

Concrete contribution to shear strength denoted in Eq. (7), depends on variables except for plastic rotation demand ($\theta_p$). One of these variables is the effective depth of RC beams ($d$). The other variables are reinforcement ratio ($\rho$), material strengths ($f_y$, $f_c$) and plastic hinge length ($L_p$). The variation of plastic hinge rotation with shear strength prediction for varying values of above-mentioned parameters is presented in Fig. 8.

## 5. Evaluation of shear strength models

Over the past few decades, many researchers have focused on shear strength degradation models for reinforced concrete. Seven existing models are selected for examination in this study. These are the ACI 318 model (2014), TEC (2007), Aschheim (1992), a model proposed by the University of California, San Diego (UCSD) (Priestley *et al*. 1994), a model proposed by the University of California, Berkeley (UCB) (Sezen *et al*. 2004), Perez (1996), and Howser (2010). The proposed equation, the requirements of two codes of practice and five equations proposed by various researchers are compared to the experimental results of this study.

### *5.1 Shear strength models*

Commentary on Building Code Requirements for Structural Concrete (ACI 318R-14) (2014) provides a conservative model for the nominal shear strength and the shear strength must exceed the shear demand $\nu_u$ as shown in Eq. (8).

$$\phi \upsilon_n \geq \upsilon_u \quad (8)$$

in which $\nu_n$ is the nominal shear strength of RC beams and has two components: the contribution of concrete $\nu_c$ and the contribution of shear reinforcement $\nu_s$ to shear strength based on yield, which is given as follows

$$\upsilon_n = \upsilon_c + \upsilon_s \quad (9)$$

For the design of new buildings, according to ACI318 (2014), the contribution of concrete to shear strength is typically simplified as follows

$$\upsilon_c = 0.17\sqrt{f_c}\left(1+\frac{N_u}{14A_g}\right) \quad (10)$$

where $N_u$ is the axial load and $A_g$ is the gross area of section.

According to the Turkish Seismic Design Code (TSDC-2007), the contribution of concrete to shear strength is mainly dependent on the compressive strength of concrete and axial load. The cracking shear strength can be calculated as

$$\upsilon_{cr} = 0.2275\sqrt{f_c}\left(1+0.07\frac{N_u}{A_g}\right) \quad (11)$$

The contribution of concrete to shear strength is determined as $\nu_c$=0.8 $\nu_{cr}$.

Aschheim and Moehle (1992) proposed that the concrete contribution to the shear strength of RC column degrades with increasing displacement ductility ($\mu_\Delta$) as follows

$$\upsilon_c = 0.3\sqrt{f_c}\left(k+\frac{N_u}{13.8A_g}\right) \quad (12)$$

where, $k$ represents the effect of displacement ductility and cannot be smaller than 0 and larger than 1.0, $N_u$ is the axial load, and $A_g$ is the gross area. This model was intended to evaluate the shear strength at plastic hinge zones, and was adopted in FEMA 273 (1997).

Priestley *et al*. (1994) suggested a relationship for predicting the concrete contribution to the shear strength of a RC column that is determined as a function of the displacement ductility as follows

$$\upsilon_c = k\sqrt{f_c} \quad (13)$$

in which $k$ depends on $\mu_\Delta$, which reduces from 0.29 in MPa units for $\mu_\Delta \leq 2$ to 0.10 in MPa units for $\mu_\Delta \leq 4$.

Sezen and Moehle (2004) proposed a shear strength model including the column aspect ratio, the axial load, the amount of shear reinforcement and the deformation ductility demand. The model take into account the apparent strength degradation associated with flexural yielding as

$$\upsilon_c = k\frac{0.5\sqrt{f_c}}{a/d}\sqrt{1+\frac{N_u}{0.5\sqrt{f_c}A_g}} \quad (14)$$

The value of $a/d$ is limited to $2 \leq a/d \leq 4$; $k$=1.0 for $\mu_\Delta \leq 2$ and $k$=0.7 for $\mu_\Delta \geq 6$ , with a linear variation between these limits.

Perez and Pantazopoulou (1996) proposed a shear strength model to define the relationship between shear strength and deformation demand through a nonlinear analytical model of cyclic plane stress states in RC. The concrete contribution to shear strength is expressed as follows

$$\upsilon_c = \frac{\alpha\rho_s}{1+\mu_\Delta}\sqrt{f_c}\left(1-\beta\frac{n}{\sqrt{f_c}}\right) \quad (15)$$

in which $\alpha$ and $\beta$ can be taken as 37 and 7.6, respectively. $\rho_s$ and $n$ are the shear reinforcement ratio and the influence of applied uniaxial stress, respectively.

Howser *et al*. (2010) conducted a parametric study on

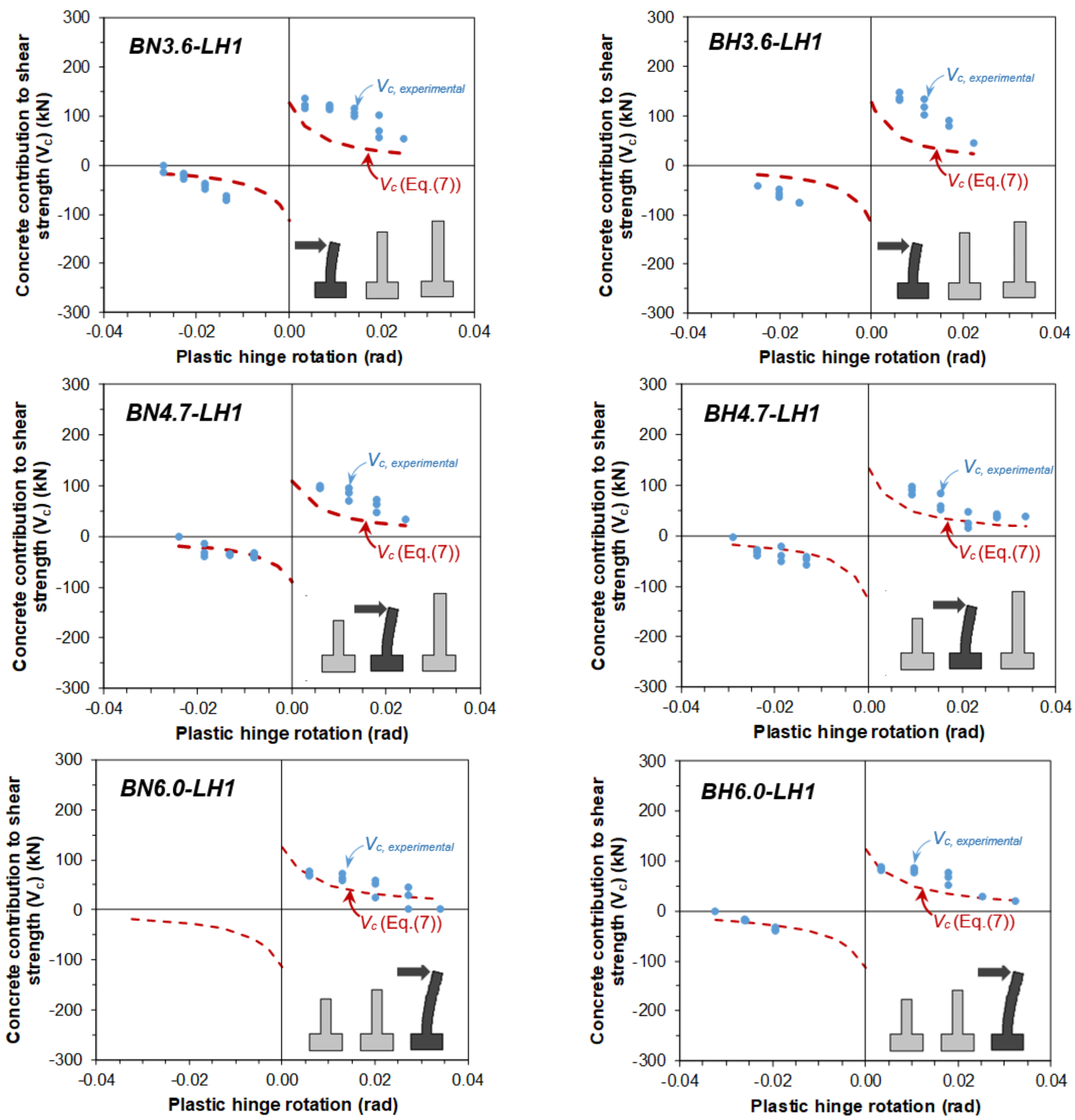


Fig. 9 Comparison of shear strength predictions using experimental results

reinforced concrete bridge piers by using a nonlinear finite element program. Based on the results of the parametric study, a relationship between flexural ductility and shear capacity of normal strength RC structures is proposed. The concrete contribution to shear strength is defined as

$$\upsilon_c = k\sqrt{f_c} \tag{16}$$

in which $k$ is a factor for influence of flexural ductility, given as $k$=0.29 for $\mu_\Delta$<2; $k$=0.29-0.12($\mu_\Delta$−2) for 2≤$\mu_\Delta$<$r$; $k$=0.53-0.095$r$-0.025$\mu_\Delta$ for $r$≤$\mu_\Delta$≤$q$; and $k$=0.53-0.095$r$-0.025$q$ for $\mu_\Delta$>$q$; $r$ is the flexural ductility at the point where the slope changes and $q$ is the flexural ductility at the point where the slope changes to zero, given as $q$=-144$\rho_s$+5.3 and $r$=-13300$\rho_s^2$+242$\rho_s$+2.8 for $\rho_s$≤0.01, $q$=$r$=3.85 for $\rho_s$≥0.01, where $\rho_s$ is the volumetric ratio of shear reinforcement.

### 5.2 Evaluation of the proposed strength model

Fig. 9 compares the shear models in terms of the impact of plastic rotation demand for all tested beams. Experimental results of concrete contribution are marked on graph beginning from displacement demand on which diagonal crack formation is observed. For samples with no diagonal crack formation, concrete contribution is not calculated/shown. With regard to the effect of plastic rotation demand, shear strength degradation initiates with the yielding of tension reinforcement. For the specimens with the shear span-to-effective depth ratio of 6 shown in Fig. 9, the proposed equation exhibits good agreement with the measured shear strengths; where the differences between the measured and calculated values are less than 10%. Considering that RC members are designed to have shear strengths much greater than their flexural strengths to ensure flexural failure according to the current codes, it is very important to have a good estimate of the proposed relationship.

Table 4 summarizes the comparisons of the concrete contribution to shear strength, $v_c$, and shear capacity, $v_n$, predictions obtained from the proposed equation, ACI318

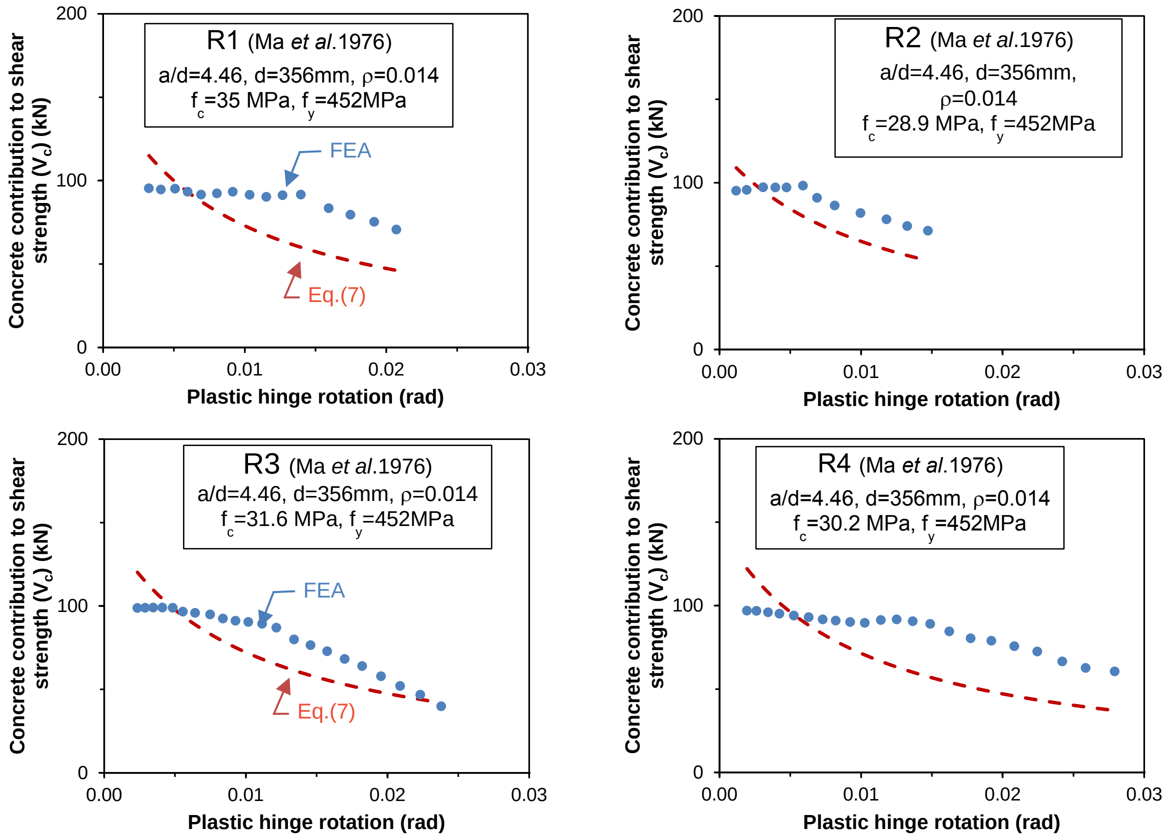


Fig. 10 Comparison of proposed shear strength (Eq. (7)) with nonlinear FEA results

Table 4 Comparison of shear strength predictions using experimental results at plastic behavior

| Prediction | Mean value (MV) | Standard deviation (SD) | Coefficient of variation (COV) |
|---|---|---|---|
| $V_{c,ACI\text{-}318}/V_{c,Experimental}$ | 3.33 | 2.40 | 0.72 |
| $V_{c,TSDC}/V_{c,Experimental}$ | 4.51 | 3.25 | 0.72 |
| $V_{c,Aschheim}/V_{c,Experimental}$ | 1.57 | 1.19 | 0.76 |
| $V_{c,Priestly}/V_{c,Experimental}$ | 1.73 | 1.26 | 0.73 |
| $V_{c,Sezen}/V_{c,Experimental}$ | 1.90 | 0.90 | 0.47 |
| $V_{c,Perez}/V_{c,Experimental}$ | 0.44 | 0.22 | 0.50 |
| $V_{c,Howser}/V_{c,Experimental}$ | 3.05 | 1.40 | 0.46 |
| $V_{c,Proposed}/V_{c,Experimental}$ | 0.70 | 0.29 | 0.42 |

(2014), TSDC (2007), Aschheim's equation (1992), Priestley's equation (1994), Sezen's equation (2004), Perez's equation (1996) and Howser's equation (2010) with the test results. The predictions by the proposed equation for the concrete contribution to shear strength of beams are relatively better, whereas Perez's equation is excessively conservative. Among the models reviewed above, TSDC (2007) and Howser *et al*. (2010) predict the highest residual shear strength of concrete at ultimate state.

In Fig. 10, concrete contribution of shear force with Eq. (7) are compared with the results of nonlinear finite element analysis of the beams. Comparisons are made for test samples named *R*1, *R*2, *R*3 and *R*4 of Ma *et al*. (1976). The general properties of test beams and the comparisons of analytical with experimental results can be found in Arslan and Kırıstioğlu (2013).

## 6. Conclusions

In this study, the concrete contribution to shear strength of ductile or nominally ductile RC beams under cyclic loading is experimentally investigated. Test program includes the comparison of test samples with varying concrete strengths, varying shear span to effective depth ratios and varying ductility level due to lateral confinement spacing. The following conclusions are drawn based on the tests and predictions of the concrete contribution to shear strength of RC beams that fail in flexure.

- Increase in *a/d* ratio of beam samples leads to not only decrease in diagonal cracking strength ($V_{cr}$) but also increase in ductility ratio at observed diagonal crack.
- Observed damages of test samples develop in the order of first crack at concrete, yield at longitudinal reinforcement, crushing at cover concrete, buckling at compression reinforcement and fracture at tension reinforcement. Concrete contribution to shear strength decreases as the damage observations become clearer during inelastic behavior for normal and high strength concrete beam samples.
- From the comparison of experimental $V_c$ values with the ones determined with assumptions independent of plastic rotation demand such as TSDC and ACI codes, it can be said that code assumptions overestimate $V_c$ values and this tendency becomes much clearer as *a/d* ratio increases.
- In order to avoid this overestimation, $V_c$ is suggested to be equal to zero independent of plastic rotation demand

for beams with reversing plastic hinge behavior. This suggestion is too conservative at the beginning of plastic behavior whereas it becomes more realistic as the plastic displacement demand increases.

• The proposed equation for the concrete contribution to shear strength displays good agreement with the measured shear strengths. Considering that RC members are designed to have shear strengths much greater than their flexural strengths to ensure flexural failure according to the current codes, it is very important to have a good estimate of the proposed relationship for beams with higher shear span-to-effective depth ratios

## Acknowledgments

This study is supported by Istanbul Aydin University Scientific Research Projects Center with the project number of BAP2015-01. The authors would like to thank Prof. Dr. A.Metin GER (KHU), Istanbul Aydın University Structural and Earthquake Engineering Laboratory staff and UTEST for their valuable contributions especially during experimental process.

## References

Acun, B. and Sucuoglu, H. (2012), “Energy dissipation capacity of reinforced concrete columns under cyclic displacements”, *ACI Struct. J.*, **109**(4), 531-540.

Arslan, G. (2005), “Shear strength of reinforced concrete frame members under cyclic loads”, Ph.D. Thesis, Yıldız Technical University, Istanbul, Turkey.

Arslan, G. and Kiristioğlu I. (2013), “Shear degradation of reinforced concrete beams”, *Eur. J. Environ. Civil Eng.*, **17**(7), 54-563. https://doi.org/10.1080/19648189.2013.799442.

Aschheim, M. and Moehle, J.P. (1992), “Shear strength and deformability of RC bridge columns subjected to inelastic displacements”, UCB/EERC 92/04, University of California, Berkeley.

Aydemir, C. and Eser Aydemir, M. (2020), “Experimental research on reversing and nonreversing plastic-hinge behavior for RC beams”, *J. Struct. Eng.*, **146**(7), 04020135. https://doi.org/10.1061/(ASCE)ST.1943-541X.0002688.

Biskinis, D.E., Roupakias, G.K. and Fardis, M.N. (2004), “Degradation of shear strength of RC members with inelastic cyclic displacements”, *ACI Struct. J.*, **101**(6), 773-783.

Bousias, S.N., Verzeletti, G., Fardis, M.N. and Guiterrez, E, (1995), “Load path effects in column biaxial bending with axial force”, *J. Struct. Eng.*, ASCE, **121**(5), 596-605. https://doi.org/10.1061/(ASCE)0733-9399(1995)121:5(596).

Collins, M.P., Bentz, E.C., Sherwood, E.G. and Xie, L. (2008), “An adequate theory for the shear strength of reinforced concrete structures”, *Mag. Concrete Res.*, **60**(9), 635-650. https://doi.org/10.1680/macr.2008.60.9.635.

De Domenico, D. and Ricciardi, G. (2020), “A stress field approach for the shear capacity of RC beams with stirrups”, *Struct. Eng. Mech.*, **73**(5), 515-527. https://doi.org/10.12989/sem.2020.73.5.515.

Elwood, K.J. and Moehle, J.P. (2005), “Axial capacity model for shear-damaged columns”, *ACI Struct. J.*, **102**(4), 578-587. https://doi.org/10.14359/14562.

FEMA 356 (1992), Concrete Chapter, California.

Keskin, R.S.O. (2017), “Predicting shear strength of SFRC slender beams without stirrups using an ANN model”, *Struct. Eng. Mech.*, **61**(5), 605-615. http://doi.org/10.12989/sem.2017.61.5.605.

Kowalsky, M.J. and Priestley, M.J.N. (2000), “Improved analytical model for shear strength of circular reinforced concrete columns in seismic regions”, *ACI Struct. J.*, **97**(3), 388-396.

Lee, J.Y. and Watanabe, F. (2003), “Shear deterioration of reinforced concrete beams subjected to reversed cyclic loading”, *ACI Struct. J.*, **100**(4), 480-489.

Ma, S.Y., Bertero, V. and Popov, E. (1976), “Experimental and analytical studies on the hysteretic behaviour of reinforced concrete rectangular and t-beams”, Tech. Rep., UBC/EERC 76-2, University of California, Berkeley.

MacGregor, G.J. (1993) ‘‘Design of slender concrete columns revisited”, *ACI Struct. J.*, **90**, 302-309.

Moehle, J., Lynn, A., Elwood, K. and Sezen, H. (2001), “Gravity load collapse of building frames during earthquakes”, PEER Report, 2nd U.S.-Japan Workshop on Performance-Based Design Methodology for Reinforced Concrete Building Structures, PEER, Richmond, California.

Mostafaei, H., Vecchio, F.J. and Kabeyasawa, T. (2009), “Deformation capacity of reinforced concrete columns”, *ACI Struct. J.*, **106**(2), 17-195. http://doi.org/10.14359/56357.

Muttoni, A. and Fernández-Ruiz, M. (2008), “Shear strength of members without transverse reinforcement as function of critical shear crack width”, *ACI Struct. J.*, **105**(2), 163-172. http://doi.org/10.14359/19731.

Olalusi, O.B. (2019), “Present state of Eurocode 2 variable strut inclination method for shear design and possible improvement”, *Struct.*, **19**, 48-57. https://doi.org/10.1016/j.istruc.2018.11.016.

Park, H.G., Yu, E.J. and Choi, K.K. (2012), “Shear-strength degradation model for RC columns subjected to cyclic loading”, *Eng. Struct.*, **34**, 187-197. https://doi.org/10.1016/j.engstruct.2011.08.041.

Paulay, T. and Priestley, M.N.J. (1992), *Seismic Design of Reinforced Concrete and Masonry Buildings*, John Wiley & Sons, Inc., New York.

Pérez, B.M. and Pantazopoulou, S.J. (1998), “Mechanics of concrete participation in cyclic shear resistance of RC”, *J. Struct. Eng.*, **124**(6), 633-641. https://doi.org/10.1061/(ASCE)0733-9445(1998)124:6(633).

Priestley, M.J.N. (2000), “Performance-based seismic design”, *Proceedings of the 12th WCEE*, Auckland.

Priestley, M.J.N., Verma, R. and Xiao, Y. (1994), “Seismic shear strength of reinforced concrete columns”, *J. Struct. Eng.*, **120**(8), 2310-2329. https://doi.org/10.1061/(ASCE)0733-9445(1994)120:8(2310).

Sezen, H. (2008), “Shear deformation model for reinforced concrete columns”, *Struct. Eng. Mech.*, **28**(1), 39-52. http://doi.org/10.12989/sem.2008.28.1.039.

Sezen, H. and Moehle, J.P. (2004), “Shear strength model for lightly reinforced concrete columns”, *J. Struct. Eng.*, **130**(11): 1692-1703. https://doi.org/10.1061/(ASCE)0733-9445(2004)130:11(1692).

Vecchio, F.J. and Collins, M.P. (1986), “The modified compression-field theory for reinforced concrete elements subjected to shear”, *ACI Struct. J.*, **83**(2), 219-231.

Zimos, D.K., Mergos, P.E. and Kappos, A.J. (2018), “Modelling of R/C members accounting for shear failure localisation: Hysteretic shear model”, *Earthq. Eng. Struct. Dyn.*, **47**, 1722-1741. https://doi.org/10.1002/eqe.3037.

*CC*